

# AUTOMATIC CHANGE DETECTION BASED ON PIXEL-CHANGE AND DSM-CHANGE

A. Sasagawa<sup>a</sup>, K. Watanabe<sup>b</sup>, S. Nakajima<sup>b</sup>, K. Koido<sup>c</sup>, H. Ohno<sup>b</sup>, H. Fujimura<sup>b</sup>

<sup>a</sup> General Affairs Dept., Geographic Survey Inst. Japan, Kitasato 1, Tsukuba, Ibaraki Pref., Japan,

<sup>b</sup> Topographic Dept., Geographic Survey Inst. Japan, Kitasato 1, Tsukuba, Ibaraki Pref., Japan,

<sup>c</sup> Tohoku Regional Survey Dept., Geographic Survey Inst. Japan, Gorin 1-3-15, Miyagino-ku, Sendai, Miyagi Pref., Japan

(sasagawa, watakin, sairo, koido, dave, hfu)@gsi.go.jp

**KEY WORDS:** Cartography, Change Detection, Pixel, Surface, Automation, Extraction

**ABSTRACT:**

A new algorithm for automatic change detection is presented. It detects a pixel-change and DSM-change from two orthoimages and two DSMs. Pixel-change is detected by using least squares fitting technique. This method performs well even if the two orthoimages have tone difference. DSM-change is detected by difference DSM. This method can detect not only constructed buildings but also features which have no changes in elevation, such as constructed roads. We have tested our method using the aerial photos observed over testfield in Tsukuba, Japan. We confirmed by the interpretation test that pixel-change and DSM-change make it easier and take less time to find changed areas even if the conditions of data acquisition are not same.

## 1. INTRODUCTION

Geographical Survey Institute (GSI) is the national mapping organization in Japan. We are now updating 1:25,000 topographic maps, which is the largest scale base map in Japan. Now GSI has two map updating policies, “rapid map revision” and “periodic revision”. In rapid map revision, we immediately update a map just after only important feature for social life is constructed such as a new highway, new land development, a reclaimed land and so on. Therefore, we always need some information about what new features are constructed. While in periodic revision, we update every feature once in several years. In this case, we need to estimate how many changes there are for our updating management.

In both policies, it is very important to find changed areas. However, now we spend much time and effort on collecting a mass of material to find changed areas. To find changed areas without difficulty, we developed the automatic change detection method based on pixel-change and DSM-change.

First we show the outline of our method. Next we describe details of each part. Then we show the result of interpretation test. We also give discussion on the features of our method.

## 2. OUTLINE

Figure 1 shows a flowchart of our method. Our method requires two orthoimages and two DSMs. Then it automatically provides “change detected image”, which is the integrated image with pixel-change image and DSM-change image. Our method contains four parts (1: georeferencing error correction, 2:pixel-change extraction, 3:DSM-change extraction, 4:image integration). Each part is described following.

## 3. METHOD

### 3.1 Georeferencing Error Correction

Georeferencing error correction is quite effective to obtain good result in pixel-change extraction and DSM-change extraction since these are quite sensitive to georeferencing errors. In this part, a georeferencing error is detected and estimated by “roughly matching” using two orthoimages. This approach estimates the relative georeferencing error between two orthoimages by using FFT (Fast Fourier Transform) every

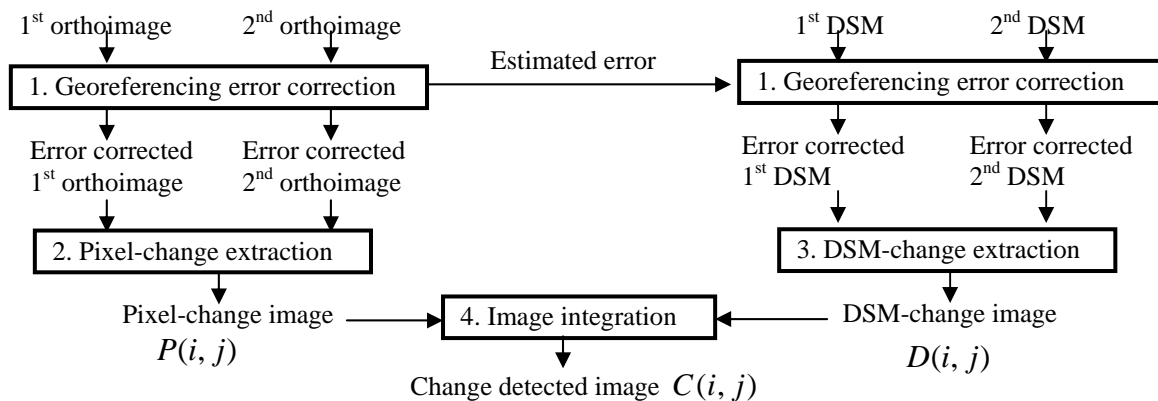


Figure 1: Flowchart of our change detection method

100 pixel square. Relative georeferencing error is corrected by the estimated georeferencing error. Error corrected DSMs are provided from this process. Also the estimated georeferencing error is applied to two DSMs.

We note that this approach can detect and estimate the relative georeferencing error, while it can not correct the absolute georeferencing error.

### 3.2 Pixel-change Extraction

Figure 2 shows a flowchart of least squares fitting technique. In this technique, following four least squares coefficients  $a, b$  for  $S_1'(i, j)$  and  $c, d$  for  $S_2'(i, j)$  are solved by using following least squares constraint equation.

$$E_1(i, j) = \text{MIN} \left[ \sum_{x=-k}^k \sum_{y=-k}^k (S_2(i+x, j+y) - S_1'(i+x, j+y))^2 \right]$$

$$E_2(i, j) = \text{MIN} \left[ \sum_{x=-k}^k \sum_{y=-k}^k (S_1(i+x, j+y) - S_2'(i+x, j+y))^2 \right]$$

Where

- $i, j$  : image coordinate
- $x, y$  : image coordinate
- $2k+1$  : window size
- $S_1(i, j)$  : pixel value of the 1<sup>st</sup> orthoimage for image coordinate  $(i, j)$
- $S_2(i, j)$  : pixel value of the 2<sup>nd</sup> orthoimage for image coordinate  $(i, j)$
- $S_1'(i, j) = aS_1(i, j) + b$
- $S_2'(i, j) = cS_2(i, j) + d$

Then E3 (absolute residual between E1 and E2) is computed.

$$E_3(i, j) = |E_1(i, j) - E_2(i, j)|$$

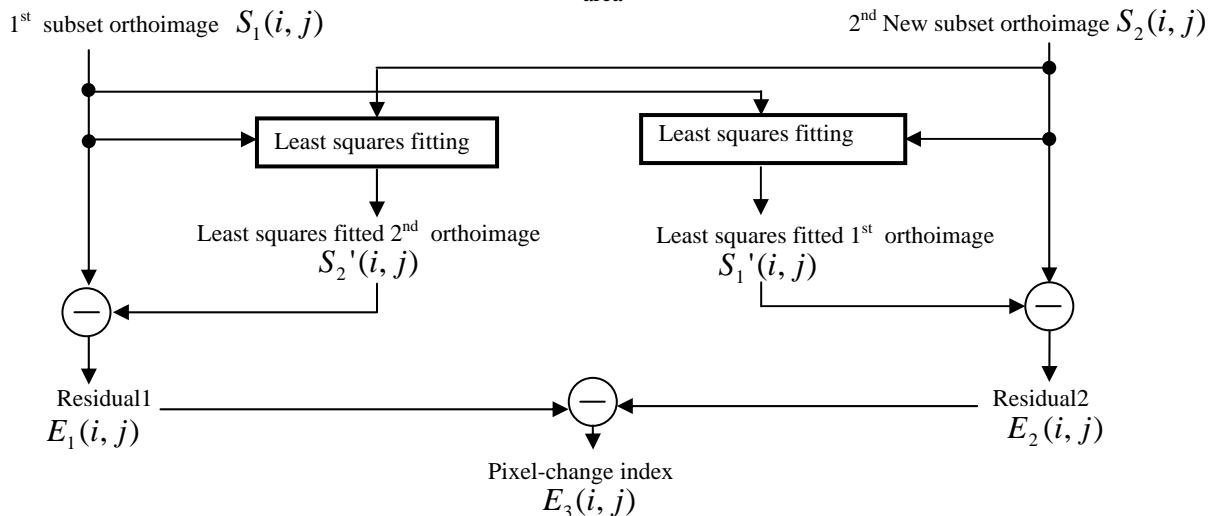


Figure 2: Flowchart of the least squares fitting technique

$S_1'(i, j)$  and  $S_2'(i, j)$  are “least squares fitted images”. In general, there must be tone difference between 1<sup>st</sup> image and 2<sup>nd</sup> image due to a difference of various conditions (used cameras, ground resolutions, acquisition date and so on). However, this technique fits a tone of 1<sup>st</sup> (2<sup>nd</sup>) image to a tone of the other image.

Figure 3 shows an example of  $S_1'(i, j)$  and  $S_2'(i, j)$  in changed area (new road is constructed). In this case,  $S_2'(i, j)$  is fitted to  $S_1(i, j)$  and it seems that least squares fitting technique performs well, while  $S_1'(i, j)$  can't be fitted completely to  $S_2(i, j)$ . Therefore  $E_1(i, j)$  gets a small value while  $E_2(i, j)$  gets a large value.

This is because the least squares fitting technique can convert high-contrast changed-images to low-contrast images, while it can't convert low-contrast images to high-contrast changed-images completely. From this asymmetric result,  $E_3(i, j)$  gets large value only in a changed area.

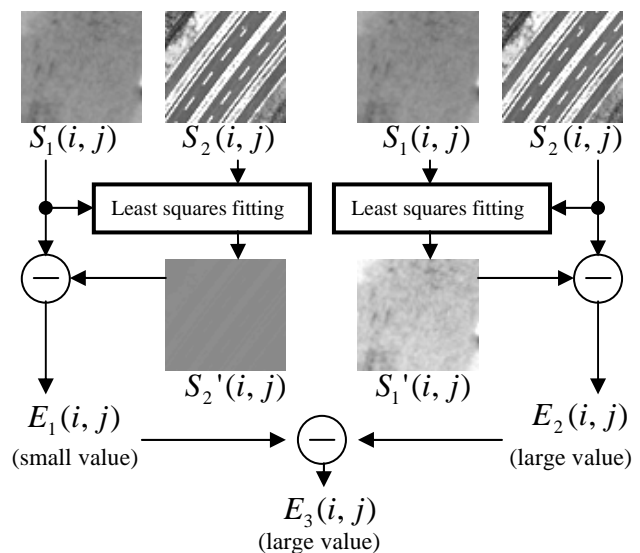


Figure 3: Example of  $S_1'(i, j)$  and  $S_2'(i, j)$  in changed area

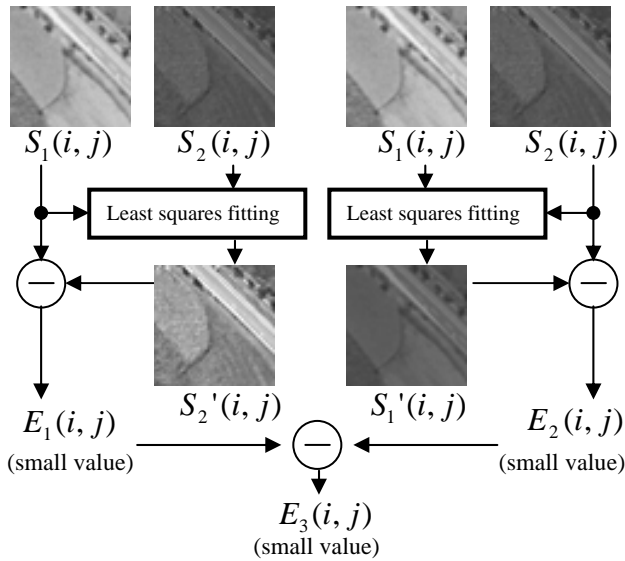


Figure 4: Example of  $S_1'(i, j)$  and  $S_2'(i, j)$  in non-changed area

Figure 4 shows an example of  $S_1'(i, j)$  and  $S_2'(i, j)$  in non-changed area. In this case, both  $S_1'(i, j)$  and  $S_2'(i, j)$  are fitted well. Therefore,  $E_1(i, j)$ ,  $E_2(i, j)$  and  $E_3(i, j)$  get a small value. Thus, even there is a tone difference between two images in a non-changed area,  $E_3(i, j)$  gets small value due to the least squares fitting technique.

Thus  $E_3(i, j)$  can be a pixel-change index for image coordinate  $(i, j)$  since it gets high value only in a changed area.

Figure 5 shows an example of a pixel-change image. A pixel-change image is generated from  $E_3(i, j)$ . As shown in Figure 5, edges only in changed areas are extracted. The quality for various conventional methods of pixel-change extraction was depended on a tone difference between two images. However, our least squares fitting technique performs well even there is a tone difference.



Figure 5: Example of pixel-change image  
 Left : 1<sup>st</sup> orthoimage  
 Center: 2<sup>nd</sup> orthoimage  
 Right : pixel-change image

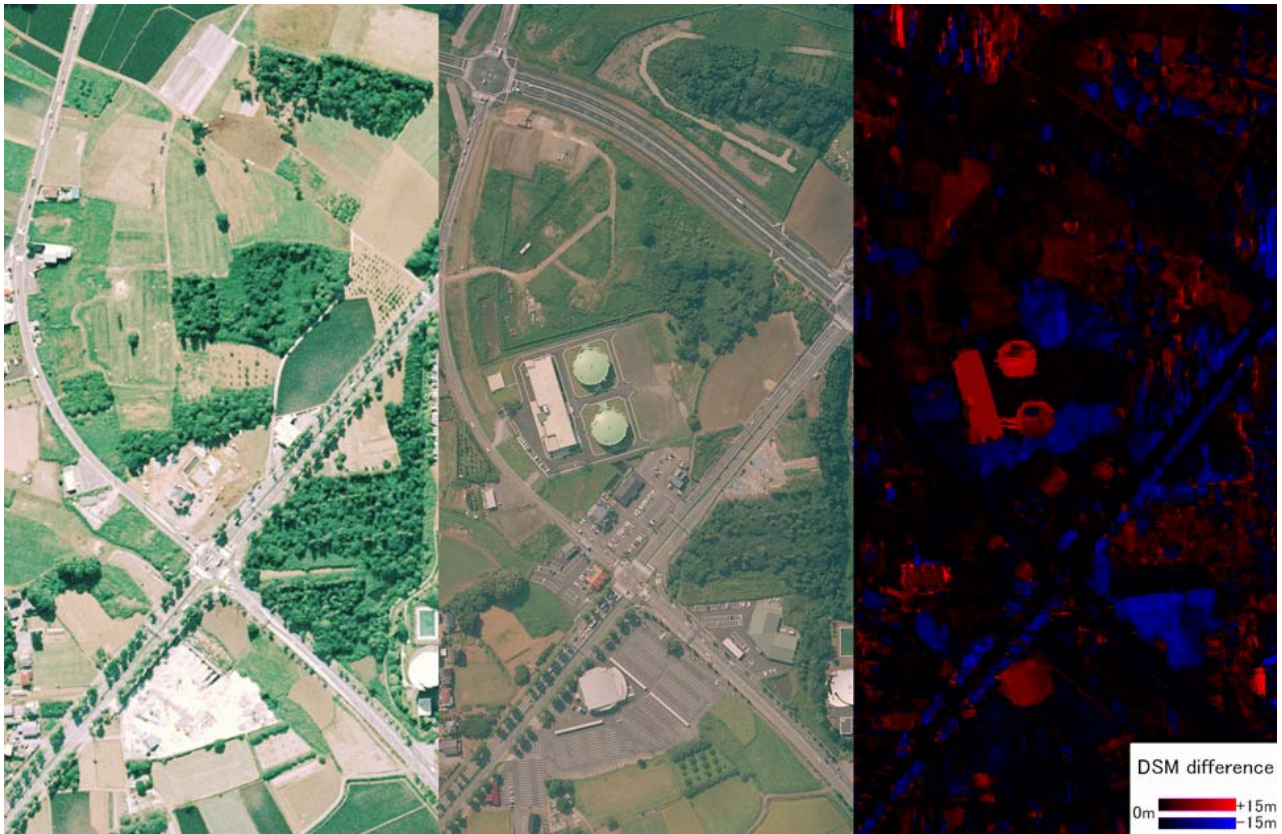


Figure 6: Example of DSM-change extraction  
 Left : 1<sup>st</sup> orthoimage  
 Center: 2<sup>nd</sup> orthoimage  
 Right : DSM-change image

### 3.3 DSM-change extraction

Figure 6 shows an example of 1<sup>st</sup> orthoimage, 2<sup>nd</sup> orthoimage and the DSM-change image. Two DSMs are computed from each pair of overlapped image. Two DSMs were given at the same grid points. Therefore DSM-change could be realized by a calculation of the vertical difference between them.

### 3.4 Image integration

Figure 7 and Figure 8 show examples of the change detected image, which is combined with a pixel-change image and a DSM-change image. Figure 7 is a subset of change detected image in Figure 8. Here, we assign the G channel to pixel-change, the R channel to positive DSM-change and the B channel to negative DSM-change. Figure 7 shows the same area for Figure 5 and Figure 6. While Figure 8 shows wider area.

### 3.5 Primary factor for quality decrease in change-detected image

We can intuitively get where the changed areas are (e.g. new buildings, new roads, cutover areas and so on) due to the both pixel-change and DSM-change. However, Figure 8 shows that pixel-change index for densely built-up area is high even it seems to be no changes. This is because an orthoimage conversion from aerial photos with DSMs is not precise enough around there. This conversion error makes a georeferencing quality worse. In such areas, pixel-change index gets high value.

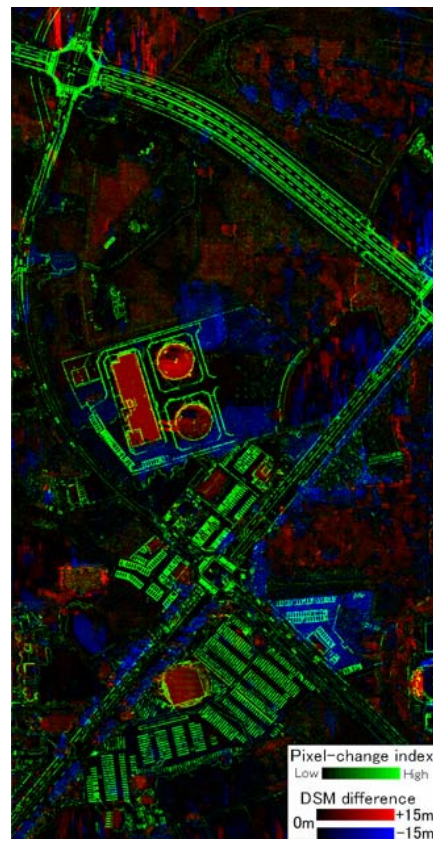


Figure 7: Example of change-detected image no.1

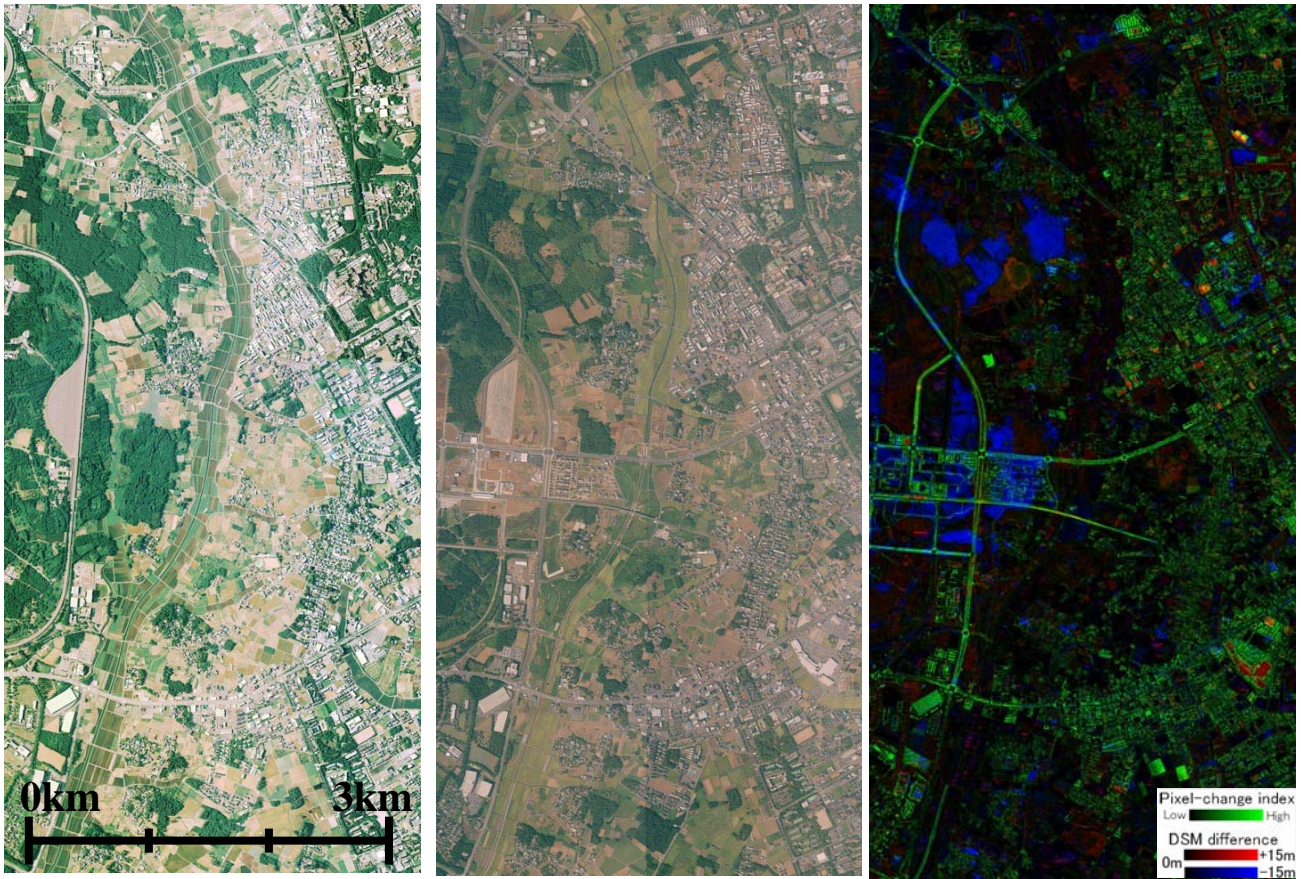


Figure 8. Example of change-detected image no.2  
 Left : 1<sup>st</sup> orthoimage  
 Center: 2<sup>nd</sup> orthoimage  
 Right : change-detected image

#### 4. INTERPRETAION TEST

We have used 2<sup>nd</sup> orthoimage, a change detected image and topographic maps which had been updated using 1<sup>st</sup> images to validate our method by an interpretation test. The specification of used aerial photos in this test is given in Table 1. Here, the 1<sup>st</sup> orthoimage, the 2<sup>nd</sup> orthoimage and the change detected image are completely same images in Figure 8. The ground resolutions are different between 1<sup>st</sup> images and 2<sup>nd</sup> images. Therefore the resolution of the 2<sup>nd</sup> images was interpolated to the resolution of the 1<sup>st</sup> images. We have compared extraction accuracy and time for finding changed areas in following two cases.

Case 1: Non professional interpreters compared the change detected image and the topographic maps to find changed areas.

Case 2: Non professional interpreters compared the 2<sup>nd</sup> orthoimage and the topographic maps to find changed areas.

The efficiency and the extraction accuracy of finding changed area in 2 cases become clear by this interpretation test. In this interpretation test, some changes (e.g. new buildings or new roads) which were not existed in both the 1<sup>st</sup> images and the topographic maps were preselected as “targets”. We measured the time and the number of targets that each interpreter had interpreted. The result of the interpretation test is given in Table

Table 1: Specification of used data

	1 <sup>st</sup> images	2 <sup>nd</sup> images
Image acquisition date	May, 1999	Sept, 2006
Image scale	1:30,000	1:8,000
Image area	24.5km <sup>2</sup> (3.5km by 7.0km)	
Ground resolution	60cm	16cm
Overlap rate (forward, side)	60%, 30%	
Exterior Orientation	58 GCPs	GPS/IMU with 5 GCPs

Table 2: Result of interpretation test

Feature (number of targets)	(case1 / case2)		
	A	B	C
New buildings (9) over 10m height	9/3	8/4	9/6
New buildings (10) under 10m height	10/3	7/4	9/3
New two-lane roads (8)	7/4	8/3	6/3
New four-lane roads (2)	2/2	2/2	2/2
New rail road (1)	1/1	1/1	1/1
Land cover change (15)	13/4	14/5	12/2
Interpretation time (min)	30/110	35/85	40/90

2. Table 2 shows the number of targets which interpreters (A, B and C) have extracted in each case. Compared with case 1, all the interpreters need less time in case 2. Nevertheless, more targets were extracted by the interpreters than in case 1. This result indicates that using a change detected images is better than using orthoimages for finding changed areas.

## **5. CONCUSION AND FUTURE WORK**

In this paper, we proposed new automatic change detection method based on pixel-change and DSM-change. We introduced "least squares fitting technique" to extract pixel-changes. This technique has robustness to the tone difference between two images. Compared with using orthoimages, using change detected images to find changed areas provides better interpretation performance and less interpretation time.

However, it becomes clear that pixel-change extraction doesn't perform so well in densely built-up area. We will study more to make it better. Also we will develop some automated method for getting an "objective change index" in each subset area using this change detection method to make an updating management easier.

## **REFERENCE**

A. Sasagawa, 2007. "Automatic Change Detection Using Pair of PRISM Triplet Images" Proc. The First Joint PI symposium of ALOS Data Nodes for ALOS Science Program in Kyoto, pp.24-38

A. Sasagawa, Y.Mizuta et al., 2007. "Study about Automatic Change Detection Using ALOS-PRISM Orthoimage (in Japanese)" Proc. 1<sup>st</sup> JSPRS Annual Conference, pp.89-90

A. Sasagawa, K.Watanabe et al., 2007. "Automatic Change Detection Using Two Aerial Photos (in Japanese)" Proc. 2<sup>nd</sup> JSPRS Annual Conference, pp.45-48

K.Watanabe, A. Sasagawa, et al., 2007. "Quality Assessment of DSM Generated by Full-Pixel Matching Technique (in Japanese)" Proc. 2<sup>nd</sup> JSPRS Annual Conference, pp.41-44

A. Gruen, S.Kocaman, K.Wolff, 2007. "CALIBRATION AND VALIDATION OF EARLY ALOS/PRISM IMAGES" Journal of the Japan Society of Photogrammetry and Remote Sensing, Vol.46, No.1, pp.24-38